Wave train generation of solitons in systems with higher-order nonlinearities

Alidou Mohamadou,[1,2,*] C. G. LatchioTiofack,[3,†] and Timoléon C. Kofané[3,‡]
[1]*Max Planck Institute for the Physics of Complex Systems, Nothnitzer Strasse 38, 01187 Dreseden, Germany*
[2]*Group of Nonlinear Physics and Complex Systems, Faculty of Science, University of Douala, P.O. Box 24157, Douala, Cameroon*
[3]*Laboratory of Mechanics, Department of Physics, Faculty of Science, University of Yaounde I, P.O. Box 812, Yaounde, Cameroon*
(Received 10 November 2009; revised manuscript received 20 April 2010; published 7 July 2010)

Considering the higher-order nonlinearities in a material can significantly change its behavior. We suggest the extended nonlinear Schrödinger equation to describe the propagation of ultrashort optical pulses through a dispersive medium with higher-order nonlinearities. Soliton trains are generated through the modulational instability and we point out the influence of the septic nonlinearity in the modulational instability gain. Experimental values are used for the numerical simulations and the input plane wave leads to the development of pulse trains, depending upon the sign of the septic nonlinearity.

DOI: 10.1103/PhysRevE.82.016601 PACS number(s): 05.45.Yv, 42.65.Tg

I. INTRODUCTION

Most of the past research interest in propagation of solitons is normally confined to Kerr media which is the manifestation of small nonlinear coefficient and nonresonant interaction. The cubic nonlinear Schrödinger (CNLS) equation has been widely used to model the propagation of light pulse in this system. However, even at the moderate pulse intensity, higher-order nonlinearities manifest themselves in a material with higher-order nonlinear susceptibilities [1]. One of the simplest case are the materials with $\chi^{(5)}$ susceptibilities which are modeling by the cubic-quintic NLS (CQNLS) equation. On the basis of experimental observations, the cubic-quintic nonlinearity was proposed as an empirical description of special glasses. In particular, in a recent experiment it has been established that the optical susceptibility of CdS_xSe_{1-x}-doped glass possesses a considerable level of fifth-order susceptibility $\chi^{(5)}$. In addition it has been further verified that there exists significant nonlinear effect due to $\chi^{(5)}$ in a transparent glass in intense femtosecond pulse at 620 nm [2]. In semiconductor double-doped optical fibers [3], the doping of silica fibers with two appropriate semiconductor particles may lead to an increased value of third-order susceptibility $\chi^{(3)}$ and a decreased value of $\chi^{(5)}$. By properly choosing the characteristics of two dopants one can choose the sign of $\chi^{(3)}$ and $\chi^{(5)}$. The saturation is also observed to increase with the reduced-photon energy. Further, experimental results of nonlinear absorption [4] in semiconductor doped glass, organic polymers and other composite materials show that nonlinearity saturates at moderate intensities. On the theoretical side, one-dimensional [5], and multidimensional [6] solitons in uniform cubic-quintic media have been studied in many works. In general a self-defocusing $\chi^{(5)}$ is needed to account for the saturation of $\chi^{(3)}$. Thus, in order to investigate pulse propagation in such materials it is necessary to consider higher-order nonlinearities in place of the usual Kerr nonlinearity. However, when the saturation is very strong, a self-focusing $\chi^{(7)}$ is also needed. Quite recently an experiment has been reported in material such as chalcogenide glass which exhibits not only third- and fifth-order nonlinearities but even seventh-order nonlinearity [7]. In other word, chalcogenide glass can be classified as a cubic-quintic-septic nonlinear material.

The above mentioned development have generated renewed interest in the investigation of optical pulse propagation in higher-order nonlinear media. In particular, the study of modulational instability (MI) in non-Kerr media has receiving particular attention. In fact, it is well established that when the input is a continuous wave (CW) light which propagates through a fiber, it can become unstable for a small perturbation under specific conditions. This is the so-called MI. The phenomenon has been observed in many branch of physics such as nonlinear optics [8,9], plasma physics [10], nonlinear electrical transmission lines [11], Bose-Einstein condensate (BEC) [12,13], biophysics [14] just to cite few. Recently, the author [15] has obtained the analytical expression for the MI gain and then numerically studied the dynamics of the solitons induced by the MI. In particular, the effects of higher-order dispersion and cubic-quintic nonlinear terms on the evolution of MI were studied. Since the nonlinearity is known to affect the MI band and the maximum gain [16], it is then important to investigate the effects of septic nonlinearity on the MI phenomenon.

In this paper we study, for the first time to our knowledge, the derivation of the MI gain in the generalized cubic-quintic-septic nonlinear Schrödinger (CQSNLS) equation with higher-order dispersion, self-steepening and Raman terms as suggested by experimental results [7]. This model is relevant to some applications in which higher-order nonlinearities are important. In particular the evolution of a soliton train induced by MI due to the effect of the new septic nonlinearity is also indicated. The paper is organized as follows: The model of equation with cubic-quintic-septic nonlinearity which describes soliton evolution in non-Kerr media with parabolic nonlinearity is discussed in Sec. II. In Sec. III, the linear stability analysis of the MI is formulated and the analytical expressions of the gain of MI is obtained. Typical outcomes of the nonlinear development of the MI, in the form of regular and irregular patterns, are reported in Sec.

*mohamali@pks.mpg.de
†glatchio@yahoo.fr
‡tckofane@yahoo.com

IV. We focus on the role played by the septic nonlinear coefficient. Section V concludes the paper.

II. MODEL

Like all electromagnetic phenomena, the propagation of optical fields in fibers is governed by Maxwell's equations. The derivation of a basic equation that governs propagation of optical pulses in CNLS equation have been obtained in [17]. Since higher-order nonlinearities manifest themselves as deviations from the cubic nonlinear response, we have modified the CNLS equation to suit with the pulse propagation in higher-order nonlinear fibers, wherein the effect of quintic and septic nonlinearities should be included. The governing equation is now called the CQSNLS equation. The CQSNLS equation can be written as follows:

$$\frac{\partial\psi}{\partial z} = i\sum_{l=1}^{l=4}\frac{i^l\beta_l}{l!}\frac{\partial^l\psi}{\partial t^l} + i\gamma_1|\psi|^2\psi + i\gamma_2|\psi|^4\psi + i\gamma_3|\psi|^6\psi + iR\psi\frac{\partial|\psi|^2}{\partial t} + S\frac{\partial(|\psi|^2\psi)}{\partial t}, \tag{1}$$

where

$$\gamma_1 = \frac{2\pi n_2}{\lambda A_{eff}}, \quad \gamma_2 = \frac{2\pi n_4}{\lambda A_{eff1}}, \quad \gamma_3 = \frac{2\pi n_6}{\lambda A_{eff2}},$$

$$S = \frac{\partial^2\beta}{\partial\omega\,\partial(|\psi|^2)}_0, \quad R = \left(\frac{\partial\beta}{\partial(|\psi|^2)_t}\right)_0 (|\psi|^2)_t. \tag{2}$$

The parameter A_{eff} is known as the effective mode area [9]. Its evaluation requires the use of its modal distribution, $F(x,y)$ for the fundamental fiber mode. Clearly, A_{eff} depends up on fiber parameters such as the core radius and the core-cladding index difference. λ is the typical wavelength for an optical fiber (λ=1.55 μm). The quantities A_{eff1} and A_{eff2} are given by

$$A_{eff1} = \frac{\left(\int\int_{-\infty}^{+\infty}|F(x,y)|^2dxdy\right)^3}{\int\int_{-\infty}^{+\infty}|F(x,y)|^6dxdy},$$

$$A_{eff2} = \frac{\left(\int\int_{-\infty}^{+\infty}|F(x,y)|^2dxdy\right)^4}{\int\int_{-\infty}^{+\infty}|F(x,y)|^8dxdy}, \tag{3}$$

where the fundamental mode $F(x,y)$ is approximated by a Gaussian distribution [17]. We obtain $A_{eff1}=(3/4)A_{eff}$ and $A_{eff2}=(1/2)A_{eff}$, where $A_{eff}=\pi w^2$. w is the width parameter of the fiber. In the following analysis we take the experimental values of the higher-order nonlinear refractive index obtained in [7] as $n_2=2.7\times10^{-13}$ cm^2/W, $n_4=-7.8\times10^{-23}$ cm^4/W, and $n_6=7.2\times10^{-33}$ cm^6/W. Thus, by choosing the effective fiber core area as $A_{eff}=40$ μm^2, we obtain the following nonlinear coefficients: $\gamma_1=2736$ W^{-1}/Km, $\gamma_2=-2.63$ W^{-2}/Km and $\gamma_3=9.2\times10^{-4}$ W^{-3}/Km.

Equation (1), which is the corresponding CQSNLS equation, models the propagation of ultrashort optical solitons in highly nonlinear single-mode fibers. It includes different effects. β_j $(j=2,3,4)$ represents, respectively, the second-order dispersion (SOD), third-order dispersion (TOD), and fourth-order dispersion (FOD). γ_1, γ_2, γ_3 are, respectively, the cubic, quintic, and septic nonlinearity. R is the intrapulse Raman scattering, which causes a self-frequency shift. S represent the self-steepening term which results from the intensity dependence of the group velocity. In practical applications the Raman and self-steepening coefficients are related to the cubic nonlinear term by $R=\gamma_1 T_R$ and $S=\gamma_1/\omega_0$ [17].

III. LINEAR STABILITY ANALYSIS

The steady-state solution of Eq. (1) can be written as

$$A(z,t) = \sqrt{P}\exp(i\phi_{NL}), \tag{4}$$

where the nonlinear phase shift ϕ_{NL} is related to the optical power P and the propagation distance as $\phi_{NL}=P(\gamma_1+P\gamma_2+P^2\gamma_3)z$. To analyze the MI of CW solution (4), we introduce the perturbed field

$$A(z,t) = [\sqrt{P} + a(t,z)]\exp(i\phi_{NL}), \tag{5}$$

where the complex field $|a(t,z)| \ll \sqrt{P}$. Thus, if the perturbed field grows exponentially, the steady state becomes unstable. By substituting Eq. (5) into Eq. (1) and collecting terms in a, we obtain the linearized equation as

$$a_z = -i\frac{\beta_2}{2}a_{tt} + \frac{\beta_3}{6}a_{ttt} + i\frac{\beta_4}{24}a_{tttt} + iP(\gamma_1 + P\gamma_2 + P^2\gamma_3)(a + a^*) + iRP(a_t + a_t^*) + SP(2a_t + a_t^*). \tag{6}$$

We assume for the perturbation $a(t,z)$, the following ansatz

$$a(t,z) = u\exp[i(Kz - \Omega t)] + v\exp[-i(Kz - \Omega t)], \tag{7}$$

where K and Ω represent, respectively, the wave number and the frequency of the modulation. Inserting Eq. (7) into Eq. (6), we obtain the dispersion relation

$$K^2 + \left(4SP\Omega - \frac{1}{3}\beta_3\Omega^3\right)K - (\beta_2P\gamma_1 + 2\beta_2P^2\gamma_2 + 3\beta_2P^3\gamma_3 - 3S^2P^2)\Omega^2 + i\beta_2RP\Omega^3 - \frac{1}{12}(3\beta_2^2 + \beta_4P\gamma_1 + 2\beta_4P^2\gamma_2 + 3\beta_4P^3\gamma_3 + 8\beta_3SP)\Omega^4 + \frac{1}{12}i\beta_4RP\Omega^5 + \left(\frac{\beta_3^2}{36} - \frac{\beta_2\beta_4}{24}\right)\Omega^6 - \frac{1}{576}\beta_4^2\Omega^8 = 0. \tag{8}$$

The dispersion relation has the following solution:

$$K(\Omega,z) = -\frac{1}{2}g_1 \pm \frac{1}{2}h_1 \pm \frac{1}{2}ih_2, \tag{9}$$

where

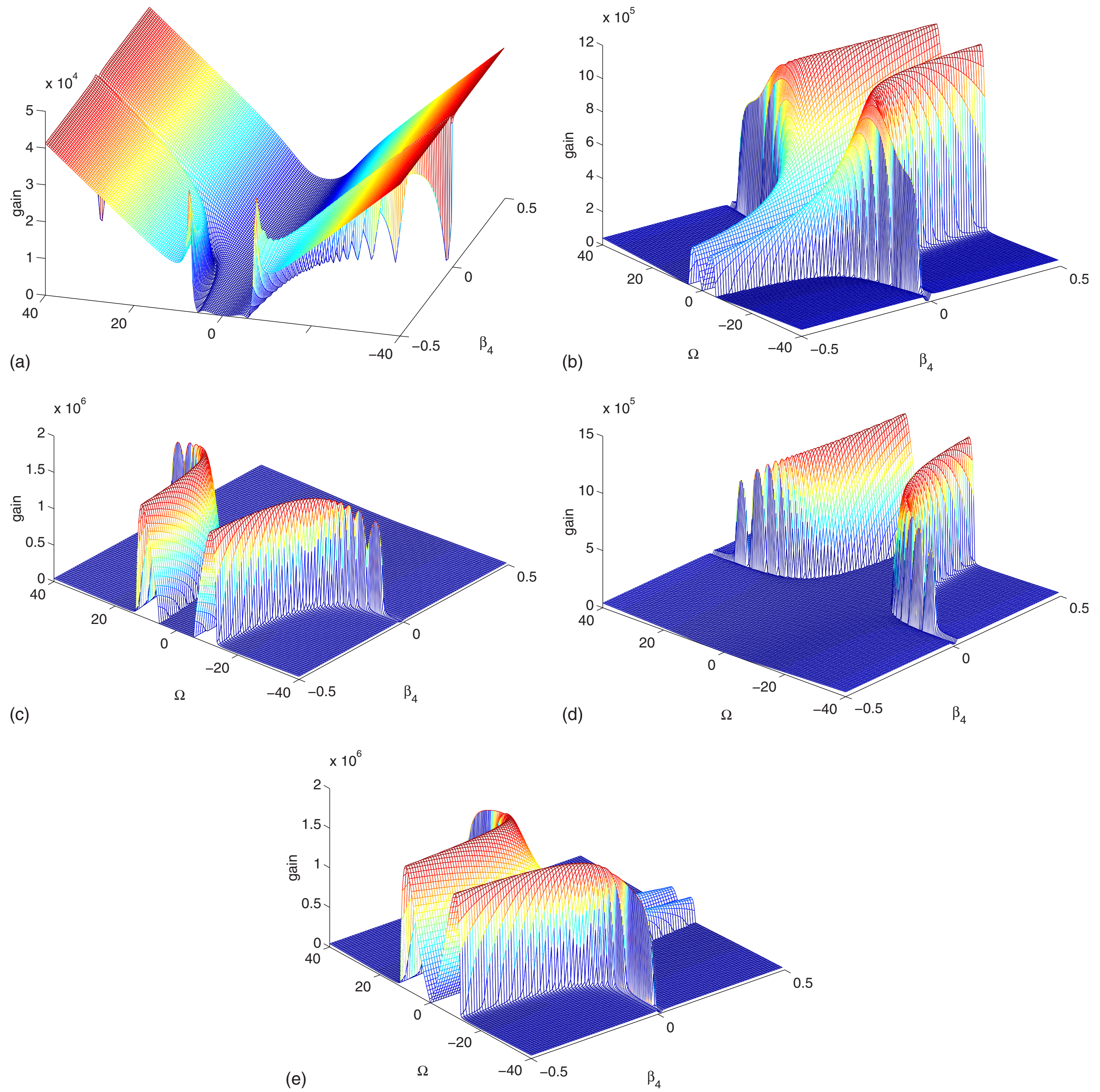

FIG. 1. (Color online) MI gain as a function of β_4 and Ω. $\gamma_1=2736\ \mathrm{W}^{-1}/\mathrm{Km}$, $\gamma_2=-2.63\ \mathrm{W}^{-2}/\mathrm{Km}$, $T_R=0.03$ fs, $P=500$ W. (a) Two gain peaks appear regardless of the sign of $\beta_2\beta_4$ and move away from the center when $\beta_4 \to 0$, $\beta_2=50\ \mathrm{ps}^2/\mathrm{Km}$, $\gamma_3=0$. (b) Two gain peaks appear when $\beta_2\beta_4>0$, while the gain disappears when $\beta_2\beta_4<0$, $\beta_2=50\ \mathrm{ps}^2/\mathrm{Km}$, $\gamma_3=-9.12\times10^{-4}\ \mathrm{W}^{-3}/\mathrm{Km}$. (c) Two gain peaks appear when $\beta_2\beta_4<0$, while the gain disappears when $\beta_2\beta_4>0$, $\beta_2=50\ \mathrm{ps}^2/\mathrm{Km}$, $\gamma_3=9.12\times10^{-4}\ \mathrm{W}^{-3}/\mathrm{Km}$. (d) Similar to (c), $\beta_2=-50\ \mathrm{ps}^2/\mathrm{Km}$, $\gamma_3=-9.12\times10^{-4}\ \mathrm{W}^{-3}/\mathrm{Km}$, (e) Similar to (b), $\beta_2=-50\ \mathrm{ps}^2/\mathrm{Km}$, $\gamma_3=9.12\times10^{-4}\ \mathrm{W}^{-3}/\mathrm{Km}$

$$g_1 = 4SP\Omega - \frac{1}{3}\beta_3\Omega^3,$$

$$h_1 = \frac{1}{2}\sqrt{\frac{\Delta_r + |\Delta|}{2}}, \quad h_2 = \frac{1}{2}\sqrt{\frac{-\Delta_r + |\Delta|}{2}},$$

$$\Delta_r = \frac{1}{4}(g_1^2 - 4L_8\Omega^8 - 4L_6\Omega^6 - 4L_4\Omega^4 - 4L_2\Omega^2),$$

$$\Delta_i=\frac{1}{4}(-4L_5\Omega^5 - 4L_3\Omega^3),$$

$$|\Delta| = \sqrt{\Delta_r^2 + \Delta_i^2}, \tag{10}$$

$$L_2 = -\beta_2 P\gamma_1 - 2\beta_2 P^2\gamma_2 - 3\beta_2 P^3\gamma_3 + 3S^2P^2, \quad L_3 = i\beta_2 RP,$$

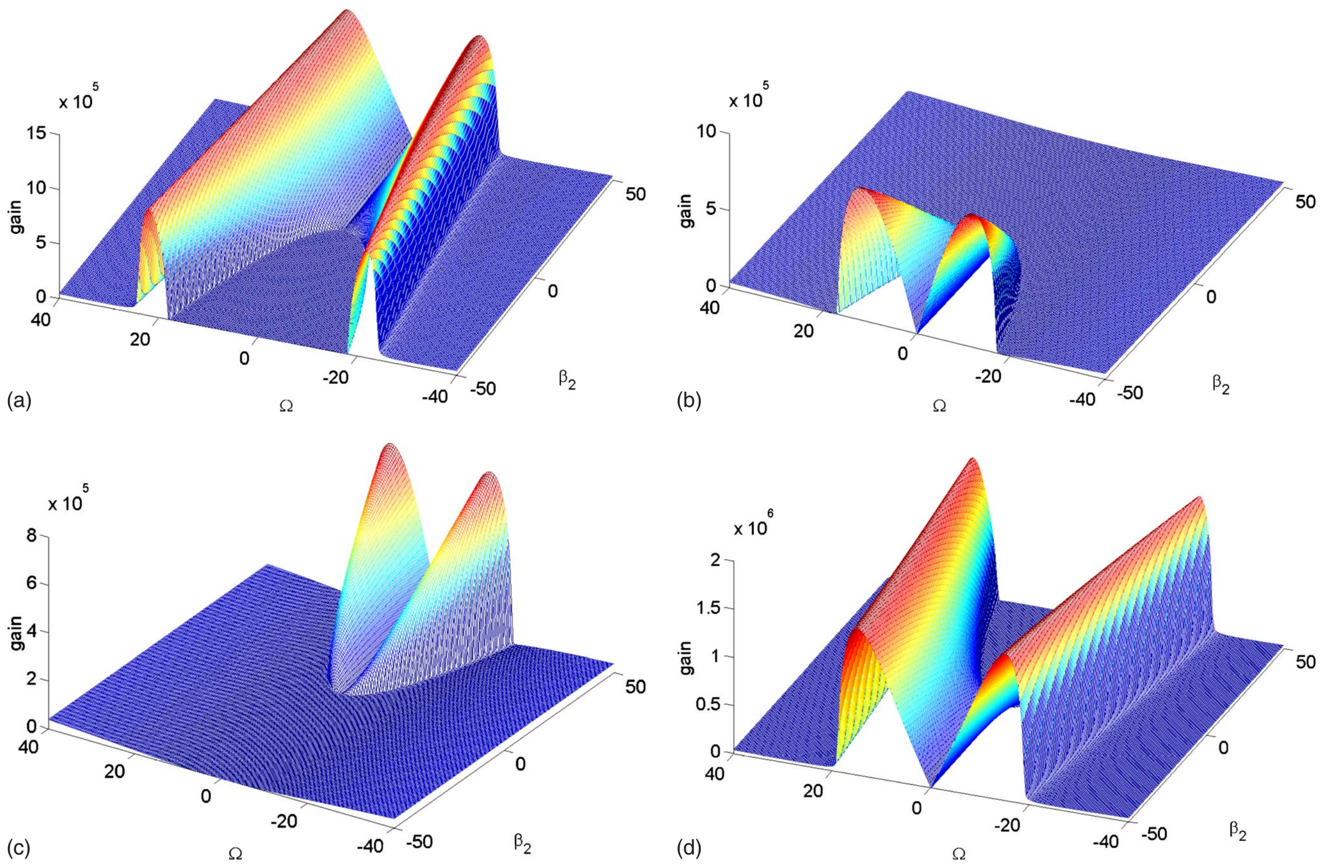

FIG. 2. (Color online) MI gain as a function of β_2 and Ω. (a) Two gain peaks appear regardless of the sign of $\beta_2\beta_4$ and move away from the center when $\beta_4 \to 0$. (b) Two gain peaks appear when $\beta_2\beta_4 > 0$, while the gain disappears when $\beta_2\beta_4 < 0$. (c) Two gain peaks appear when $\beta_2\beta_4 > 0$, while the gain disappears when $\beta_2\beta_4 < 0$. (d) Similar to (a).

$$L_4 = -\frac{1}{12}(3\beta_2^2 + \beta_4 P\gamma_1 + 2\beta_4 P^2\gamma_2 + 3\beta_4 P^3\gamma_3 + 8\beta_3 SP),$$

$$L_5 = \frac{1}{12} i\beta_4 RP,$$

$$L_6 = \frac{\beta_3^2}{36} - \frac{\beta_2\beta_4}{24}, \quad L_8 = -\frac{1}{576}\beta_4^2. \tag{11}$$

The steady-state solution becomes unstable whenever K has an imaginary part. The perturbation then grows exponentially with the intensity given by the growth rate of the MI gain defined as: $g(\Omega)=2|Im(K)|$ [9,17]. Hence we have

$$g(\Omega) = \sqrt{\frac{-\Delta_r + |\Delta|}{2}}. \tag{12}$$

Now we investigate the impact of the septic nonlinearity in the gain spectra. Figure 1(a) shows the MI gain as a functions of β_4 and Ω in the normal dispersion regime in the absence of the septic nonlinearity. In the case of a negative value of the septic term γ_3, we obtain the gain spectrum having two distinct side lobes in Fig. 1(b), which exist regardless of the sign of the FOD β_4. We note also that the maximum gain increases when $\beta_4 > 0$. In the case of a positive value of the septic nonlinearity, Fig. 1(c) shows that the gain spectrum also has two distinct side lobes, but, as compared with Fig. 1(b), the side lobes vanish when $\beta_4 > 0$. Figures 1(d) and 1(e) plot the gain spectra for the anomalous dispersion regime. In Fig. 1(d) we observe two similar side lobes as in Fig. 1(c), but the two side lobes vanish here when $\beta_4 < 0$. On the other hand we observe in Fig. 1(e) that the two side lobes exist regardless of the sign of the FOD, but, as compared with Fig. 1(b), the maximum gain decreases when $\beta_4 < 0$.

Figure 2 displays the MI gain as function of β_2 and Ω with fixed β_4 and P. In the case of negative value of the septic term γ_3, we obtain two side lobes in Fig. 2(a) which exist regardless of the sign of the product $\beta_2\beta_4$. In the case of positive value of the septic terms γ_3, we observe that the space between the two sidebands is reduced progressively when β_2 increases. The nonzero gain peaks appear only if $\beta_2\beta_4 > 0$. The gain spectrum in Fig. 2(c) is similar to Fig. 2(b). Finally, Fig. 2(d) presents also two side lobes as in Fig. 2(a), but here, the space between the two sidebands is enhanced progressively when β_2 increases.

We can then conclude that the gain is sensitive to the septic nonlinearity. It should be emphasized that the linear stability analysis is valid as long as the perturbation amplitude remains small compared with the CW beam amplitude. If the perturbation amplitude grows large enough to be comparable to that of the incident CW beam, the numerical analysis must be adapted.

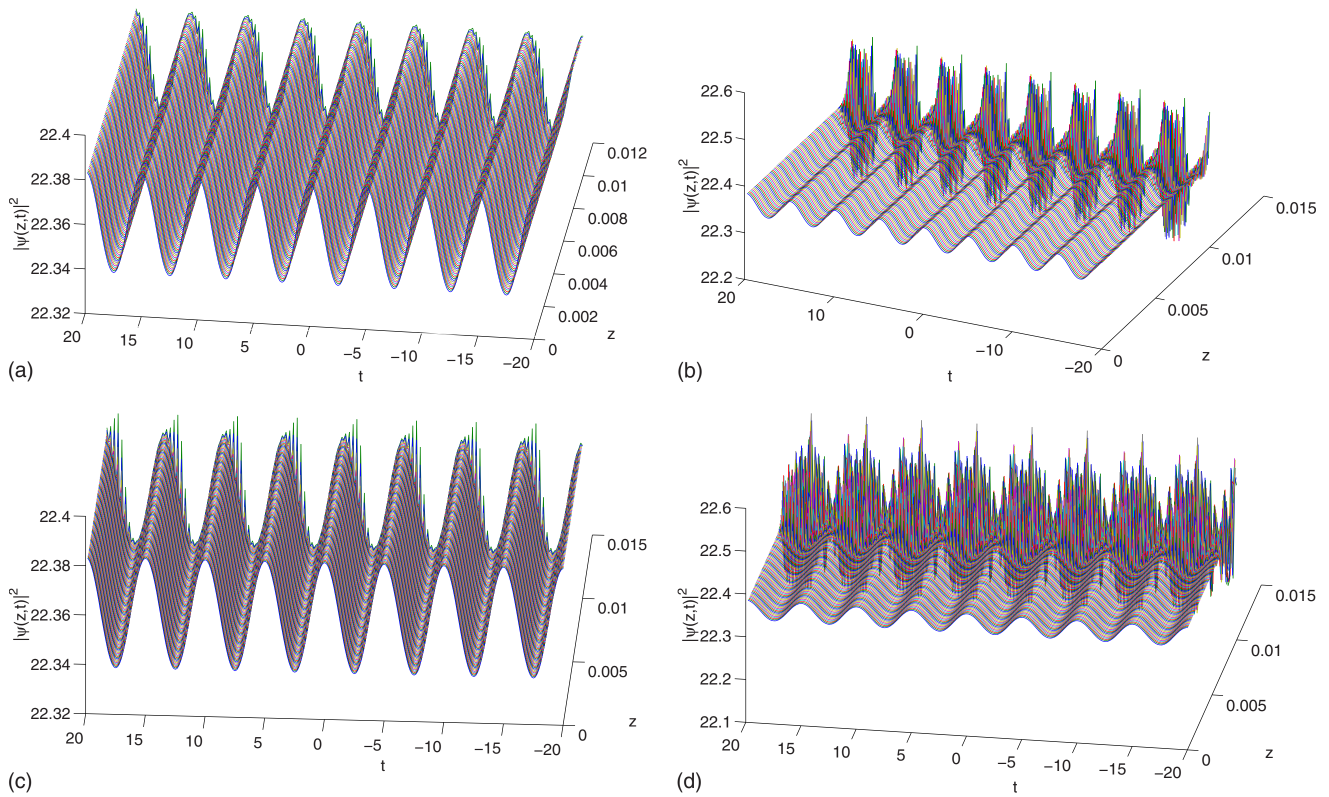

FIG. 3. (Color online) Evolution of CW showing the effects of the septic nonlinear term. (a) $\beta_4=0.05$ ps^4/Km, $\beta_2=50$ ps^2/Km, $\gamma_3=0$, (b) $\beta_4=0.05$ ps^4/Km, $\beta_2=50$ ps^2/Km, $\gamma_3=9.12\times10^{-4}$ W^{-3}/Km, (c) $\beta_4=0.05$ ps^4/Km, $\beta_2=-50$ ps^2/Km, $\gamma_3=0$, (d) $\beta_4=-0.05$ ps^4/Km, $\beta_2=-50$ ps^2/Km, $\gamma_3=9.12\times10^{-4}$ W^{-3}/Km.

IV. NUMERICAL SIMULATIONS

The next step of the analysis is to run a direct simulation of Eq. (1), adding small initial modulational perturbations to CW states with the objective to identify nonlinear patterns generated by the MI. The MI is induced by injecting an input signal in the form [9,17]

$$\psi(0,t)=\sqrt{P}[1+a_m\sin(2\pi\Omega_m t)]\exp(i\phi_{NL}), \qquad (13)$$

where $a_m=0.001$ is the modulation amplitude and $\Omega_m=0.2$ is the frequency of a weak sinusoidal modulation imposed on the CW beam. Equation (1) with initial condition [Eq. (13)] is solved utilizing the split-step fourier method [9,17].

As an example, we consider the case $\beta_2=50$ ps^2/Km, $\beta_3=0.04$ ps^3/Km, $\beta_4=0.05$ ps^4/Km, $\gamma_1=2760$ W^{-1}/Km, $\gamma_2=-2.63$ W^{-2}/Km, $\gamma_3=-9.12\times10^{-4}$ W^{-3}/Km and $T_R=0.03$ fs, which belong to the coefficients of the MI spectrum in Fig. 1. Figures. 3(a) and 3(c) plot the evolution of the amplitude of the CW state when the septic nonlinearity is set to zero. In the absence of septic nonlinearity the outcome is generation of a regular array of localized peaks and leads to the establishment of a periodic-train of solitary pulses, its period which is the same as imposed by the initial modulational perturbation. Obviously this solution is of direct interest to applications in terms of the generation of a pulse array in fiber lasers, but, as shown in Fig. 3(b), the presence of the septic nonlinearity could influence the evolution of the periodic soliton. The initially perturbed CW is stable at the initial stage of the evolution, but after certain propagation distance we observed that the train of solitons turns into a chaotic pulse. Figures 3(c) and 3(d) plot the evolution of the peak power in the case of anomalous dispersion regime. The results are similar to the case of normal dispersion [Figs. 3(a) and 3(b)]. We can then conclude that the septic nonlinearity influences the evolution of the train of solitons.

V. CONCLUSION

In this work we have used the higher-order nonlinear Schrödinger equation with cubic-quintic-septic nonlinearity, modeling the propagation of an ultrashort femtosecond optical pulses. An analytic expression for the MI gain have been obtained and shown to be sensitive of the septic nonlinearity. Direct simulations of the CQSNLS equation have been performed. The outcomes of the instability development depend up on the septic nonlinearity. The results, especially the formation of the stable periodic array of localized pulses, may find straightforward applications in nonlinear optics.

ACKNOWLEDGMENTS

A.M. is grateful for the hospitality of the Max-Planck Institute for the Physics of Complex Systems in Dresden.

[1] J. L. Coutaz and M. Kull, J. Opt. Soc. Am. B **8**, 95 (1991); P. Roussignol, D. Richard, J. Lukasik, and C. Flytzanis, *ibid.* **4**, 5 (1987).
[2] Z. Jovanoski and D. R. Roland, J. Mod. Opt. **48**, 1179 (2001).
[3] S. Gatz and J. Herrmann, Opt. Lett. **17**, 484 (1992); H. Yanay, L. Khaykovich, and B. A. Malomed, Chaos **19**, 033145 (2009).
[4] G. I. Stegeman and R. H. Stolen, J. Opt. Soc. Am. B **6**, 652 (1989).
[5] F. Kh. Abdullaev and J. Garnier, Phys. Rev. E **72**, 035603(R) (2005); V. Prytula, V. Vekslerchik, and V. M. Perez-Garcia, *ibid.* **78**, 027601 (2008); H. Leblond, B. A. Malomed, and D. Mihalache, *ibid.* **71**, 036608 (2005).
[6] M. J. Paz-Alonso and H. Michinel, Phys. Rev. Lett. **94**, 093901 (2005); B. A. Malomed, L.-C. Crasovan, and D. Mihalache, Physica D **161**, 187 (2002); H. Michinel, J. R. Salgueiro, and M. J. Paz-Alonso, Phys. Rev. E **70**, 066605 (2004).
[7] Y. Chen, K. Beckwitt, F. Wise, B. Aitken, J. Sanghera, and I. D. Aggarwal, J. Opt. Soc. Am. B **23**, 347 (2006).
[8] W. P. Hong, Opt. Commun. **213**, 173 (2002); F. II. Ndzana, A. Mohamadou, and T. C. Kofane, *ibid.* **275**, 421 (2007).
[9] G. P. Agrawal, *Nonlinear Fiber Optics*, Optics and Photonics, 4th ed. (Academic Press, New York, 2009).
[10] I. Kourakis and P. K. Shukla, Phys. Plasmas **11**, 1384 (2004).
[11] F. II Ndzana, A. Mohamadou, and T. C. Kofane, Phys. Rev. E **79**, 056611 (2009); M. Remoissenet, *Waves Call Solitons*, 3rd ed. (Springer, Berlin, 1999).
[12] L. Salasnich, A. Parola, and L. Reatto, Phys. Rev. Lett. **91**, 080405 (2003); S. L. Cornish, S. T. Thompson, and C. E. Wieman, *ibid.* **96**, 170401 (2006).
[13] G. Theocharis, Z. Rapti, P. G. Kevrekidis, D. J. Frantzeskakis, and V. V. Konotop, Phys. Rev. A **67**, 063610 (2003); E. Wamba, A. Mohamadou, and T. C. Kofane, Phys. Rev. E **77**, 046216 (2008).
[14] C. B. Tabi, A. Mohamadou, and T. C. Kofane, J. Phys.: Condens. Matter **20**, 415104 (2008).
[15] W. P. Hong, Naturforscher **61a**, 225 (2006).
[16] M. L. Lyra and A. S. Gouveia Neto, Opt. Commun. **108**, 117 (1994).
[17] G. P. Agrawal, *Nonlinear Fiber Optics* (Academic, Boston, 1989).